Theory of Sub-keV Photoionization Cross Sections

Steven T. Manson

Citation: AIP Conference Proceedings **75**, 156 (1981); doi: 10.1063/1.33162
View online: https://doi.org/10.1063/1.33162
View Table of Contents: http://aip.scitation.org/toc/apc/75/1
Published by the American Institute of Physics

Theory of Sub-keV Photoionization Cross Sections

Steven T. Manson
Department of Physics and Astronomy, Georgia State University
Atlanta, Georgia 30303

ABSTRACT

An overview of the calculation of photoionization cross sections for $h\nu < 1$ keV is presented with particular emphasis on providing a guide for evaluating the accuracy of theoretical work. An attempt is made to focus upon the various approximations made in each level of calculation and point out in which ranges they should be good. Central-field, Hartree-Fock, and more sophisticated methods are reviewed, particularly as they apply to free atoms and ions. In addition, the striking similarity of such calculated cross sections to core level photoemission in solids is pointed out.

I. INTRODUCTION

The photoelectric effect, which is the overwhelmingly predominant mechanism of absorption of $h\nu \lesssim 1$keV electromagnetic radiation by matter, was one of the earliest harbingers of the breakdown of classical physics. Its discovery, well back in the nineteenth century, was followed by the explanation of the phenomenon in 1905 by Einstein.[1] By the end of the 1920's, with the Schrödinger and Dirac equations on firm ground, the basic theory of photoionization was worked out. An excellent review which includes this theory was written in 1933 by Bethe[2]; a slightly later one on photoionization exclusively was written in 1936 by Hall.[3]

Once the theory was set down, the problem of calculating photoionization cross sections became one of obtaining wave functions for the initial discrete and final continuum states of the system. For the hydrogen atom this can be done exactly, but for many electron systems, it cannot. The thrust of this paper, then, is to go through various of the methodologies employed for obtaining photoionization cross sections theoretically with particular emphasis on the physical approximations made at each level of calculation as well as an estimate of the accuracy of each level along with the energy range in which is expected to be useful. This is done in an effort to give experimentalists and "consumers" of such calculations the tools to assess the accuracy of published results since theoretical papers rarely, if ever, include error bars.

The literature in this field is considerable and it would be a tremendous task to attempt to give references to all of the relevent papers. Thus indicative examples, rather than complete coverages, are aimed at. In addition, references are made to other reviews, where possible, in an attempt to give access to as much of the extant literature as possible.

In this paper we shall restrict out attention to the calculation of total and subshell cross sections for free atoms and ions. Some comments shall be made about the applicability of such results to solids, however. Photoelectron angular distributions shall be omitted entirely; for reviews on that subject, see Refs. 4-8.

II. GENERAL THEORY OF PHOTOIONIZATION CROSS SECTIONS

In the photoionization process, a photon of energy $h\nu$ collides with a target in state i and gets absorbed, its energy going to an electron which is ejected leaving the residual ion in state j, i.e.,

$$h\nu + A(i) \rightarrow A(j)^+ + e^-. \qquad (1)$$

Usually i and j refer to the ground states of A and A^+ respectively, but they may, in principle, be excited states as well. The fundamental relationship for the energetics is a photoionization process as given by[9]

$$\varepsilon = h\nu - I_{ij} \qquad (2)$$

where ε is the kinetic energy of the photoelectron and I_{ij} is the ionization energy.

The photoionization cross section for a system in state i by an unpolarized photon beam of energy $h\nu$ leaving the system in a final state f consisting of a photoelectron of energy ε plus ions in state j is given by[9]

$$\sigma_{ij}(\varepsilon) = (4\pi^2\alpha a_0^2/3g_i)(\varepsilon + I_{ij})|M_{if}|^2 \qquad (3)$$

where α is the fine structure constant (1/137), a_0 is the Bohr radius (5.29×10^{-9} cm). g_i is the statistical weight of the initial discrete state, and the ionization energy I_{ij} and the photoelectron energy ε are expressed in Rydbergs (13.6 eV). The matrix element, expressed in Rydberg atomic units, is given by[10]

$$|M_{if}|^2 = \frac{4}{(I_{ij} + \varepsilon)^2} \sum_{i,f} \left| \langle f | \sum_\mu \exp(i\vec{k}_\nu \cdot \vec{r}_\mu) \vec{\nabla}_\mu | i \rangle \right|^2, \qquad (4)$$

with the summation over i,f being the sum over the degenerate initial and final states respectively, $\vec{r}_\mu$ is the position coordinate of the μth electron, $\vec{k}_\nu$ is the propagation vector of the photon ($|\vec{k}_\nu| = 2\pi\nu/c$), and the wave functions are normalized such that for the initial discrete state $|i\rangle$

$$\langle i | i \rangle = 1, \qquad (5)$$

and for the final continuum state $|f\rangle$ (= $|j,\varepsilon\rangle$)

$$\langle j,\varepsilon | j',\varepsilon' \rangle = \delta_{jj'}\, \delta(\varepsilon - \varepsilon'). \qquad (6)$$

Up to this point the theory is essentially exact. By "essentially" is meant that Eq. (3) is really a first-order perturbation theory.[11] It is to be noted, however, that the second-order perturbation result is a factor of α (1/137) smaller than the first-order. Thus, it is an excellent approximation to neglect it and all higher order contributions.

In addition, for incident photon energies below several keV, the $\exp(i\vec{k}_\nu \cdot \vec{r}_\mu)$ term in the matrix element Eq. (4) can be approximated. This is done by noting that the major concentration of wave function amplitude is around a distance from the nucleus, $\vec{r}_\mu$, of the order of the Bohr radius. Thus, for photon energies below several keV, $\vec{k}_\nu \cdot \vec{r}_\mu$ is small enough so that $\exp(i\vec{k}_\nu \cdot \vec{r}_\mu)$ can be approximated very well by unity. Actually, the approximation for cross sections is much better than is implied by the discussion. This is because expanding the exponential out gives $1 + i\vec{k}_\nu \cdot \vec{r}_\mu$ and taking the absolute square yields $1 + (\vec{k}_\nu \cdot \vec{r}_\mu)^2$ so we really need have only $(\vec{k}_\nu \cdot \vec{r}_\mu)^2$ very small compared to unity for the approximation to be valid. This approximation simplifies the matrix element considerably and is known as the "dipole approximation" or "neglect of retardation." The matrix element M_{ij} can then be written[10]

$$M_{if} = \frac{4}{(I_{ij} + \varepsilon)^2} \sum_{if} \left| \langle f | \sum_\mu \vec{\nabla}_\mu | i \rangle \right|^2 = \sum_{if} \left| \langle f | \sum_\mu \vec{r}_\mu | i \rangle \right|^2, \qquad (7)$$

and it is seen that the problem of calculation of photo-

0094-243X/81/750156-06$1.50

ionization cross sections reduces to one of finding wave functions for initial and final states. The details of the transformation of the matrix element in Eq. (7) are given elsewhere.[4,6,10]

The first expression in Eq. (7) is known as the dipole-velocity (or just "velocity") form of the matrix element while the last is the dipole-length (often referred to as "length"). These two alternate forms of the matrix element (actually there are others which are used infrequently in practice[4,6,10]) are shown to be equal when exact wave functions are used.

Of course, for atomic systems other than hydrogen, exact wave functions are not available. In the case of approximate wave functions, the results of using the various expressions for the dipole matrix element can differ considerably from each other and from the correct answer. On the other hand, it is possible that both expressions might give the same result with approximate wave functions, and that this result might still be incorrect. This point will be discussed further in connection with central field wave functions below. We thus see that equality among the results of the alternative forms of the dipole matrix element is a necessary but not sufficient condition for the correctness of that result. The question as to which form of the matrix element should be more accurate has been discussed,[12-15] but no definitive conclusion has been reached.

III. CENTRAL FIELD CALCULATIONS

The simplest type of wave functions which are useful in calculating photoionization cross sections are those based on a central-field approximation to the exact Hamiltonian, i.e., one considers the solution to the approximate Hamiltonian

$$H_0 = \sum_\mu [(P_\mu^2/2m) + U(r_\mu)] \tag{8}$$

for the initial and final states of the atom or ion. Note that $U(r_\mu)$, the central potential seen by each electron, is a function of scalar r_μ only. The solutions to H_0 are antisymmetric products of one-electron wave functions, $r^{-1}P_{n\ell}(r)Y_\ell^m(\theta,\phi)$ [$r^{-1}P_{\varepsilon\ell}(r)Y^m(\theta,\phi)$ for continuum electrons]. The radial parts of the one-electron functions are solutions to the one-body Schrödinger equation

$$\left[\frac{d^2}{dr^2} - \frac{\ell(\ell+1)}{r^2} - U(r) + E\right]P(r) = 0 \tag{9}$$

for both discrete and continuum functions. Eq. (9) has r in atomic units and energies in Rydbergs. In using central-field wave functions, then, only the one electron is permitted to change quantum numbers in the photoionization process or the matrix element vanishes. Thus, multiple transitions are specifically excluded. Further, since the initial and final states are solutions to the Schrödinger equation in the same central U(r), the orbitals not directly involved in the photoionizing transition remain unchanged. The rearrangement of the remaining electrons after a transition is known as core relaxation, i.e., core relaxation effects are excluded in the central-field model. Therefore, the nonparticipating orbitals integrate out to unity in the dipole matrix element and the photoionization cross section for an nl electron can be written in dipole-length form as[16]

$$\sigma_{n\ell}(\varepsilon) = \frac{4}{3}\pi^2\alpha a_0^2 \frac{N_{n\ell}(\varepsilon - \varepsilon_{n\ell})}{2\ell+1}[\ell R_{\ell-1}(\varepsilon)^2 + (\ell+1)R_{\ell+1}(\varepsilon)^2], \tag{10}$$

with $\varepsilon_{n\ell}$ the binding energy of an nl electron (explicitly negative), $N_{n\ell}$ the occupation number of the nl subshell, and the matrix element

$$R_{\ell\pm1}(\varepsilon) = \int_0^\infty P_{n\ell}(r) r P_{\varepsilon,\ell\pm1}(r)dr, \tag{11}$$

where the continuum normalization, from Eq. (6) takes the form

$$P_{\varepsilon\ell}(r) \xrightarrow[r\to\infty]{} \pi^{-\frac{1}{2}}\varepsilon^{-\frac{1}{4}}\sin[\varepsilon^{\frac{1}{2}}r - \tfrac{1}{2}\ell\pi - \varepsilon^{-\frac{1}{2}}\ln 2\varepsilon^{\frac{1}{2}}r + \sigma_\ell(\varepsilon) + \delta_\ell(\varepsilon)], \tag{12}$$

where $\sigma_\ell(\varepsilon) = \mathrm{Arg}\,\Gamma(\ell + 1 - i\varepsilon^{-\frac{1}{2}})$ and $\delta_\ell(\varepsilon)$ is the is the phase shift. It is thus seen that the central-field calculation reduces the problem to a one-electron model of the photoionization process involving only the wave function of the photoelectron before and after the photoionization, and a single-electron Hamiltonian

$$h_0 = (P^2/2m) + U(r) \tag{13}$$

to which each is a solution.

An interesting property of the one-electron model is that the various alternative forms of the dipole matrix element, discussed above, must be equal[14] which shows that equality of "length" and "velocity" is no guarantee of agreement with experiment. In the central field case the alternative forms of the dipole matrix element, then, give no information as to how close to experiment the results of a central-field calculation are. They do, however, provide a powerful check on the numberical methods used in the computation. It is almost impossible, for example, to have an error in the calculation of the dipole matrix element and still retain the equality of length and velocity.

Up to this point, the detailed form of the central potential has not been dealt with. A number of choices exist and discussion of them is treated elsewhere.[4] It must be pointed out, however, that a reasonable potential must have the correct boundary conditions

$$U(r) \xrightarrow[r\to0]{} -2Z/r,\quad U(r) \xrightarrow[r\to\infty]{} -2/r, \tag{14}$$

in Rydbergs. A number of such potentials have been used but the most common is the Hartree-Slater (HS) potential[17,18] with which numerous calculations have been performed for both atoms[4-7,19,20] and ions.[21]

The strengths and weaknesses of such an approach can best be spotlighted by examples. In Fig. 1, the calculated total photoionization cross section for xenon[19] from threshold to above 1 keV is shown, along with experimental results.[22-24] From this figure, very good overall agreement in general shape is found. In addition away from the 5p and 4d ($N_{4,5}$) thresholds, quantitative agreement is pretty good as well. Near those thresholds, however, there are discrepancies between the central field calculation and experiment which are as large as a factor of two.

Fig. 1 also exhibits some of the important features of photoionization cross sections.[25] One is the fact that each subshell cross section does not necessarily decrease monotonically from threshold. These maxima above threshold are called delayed maxima[19] and are caused by the angular momentum barriers in the $n\ell \to \varepsilon\ell+1$ photoionization channels. The effective potential, as seen by the continuum electron, has a repulsive centrifugal term which keeps the $\ell+1$ continuum wave function very small in the core region near threshold. Thus the overlap with the bound state wave function is small, making the matrix element small and, thereby, the cross section small. With increasing energy, however, the continuum wave function begins to penetrate the barrier, increasing the overlap and increasing the cross section above the threshold value. As an example, the wave

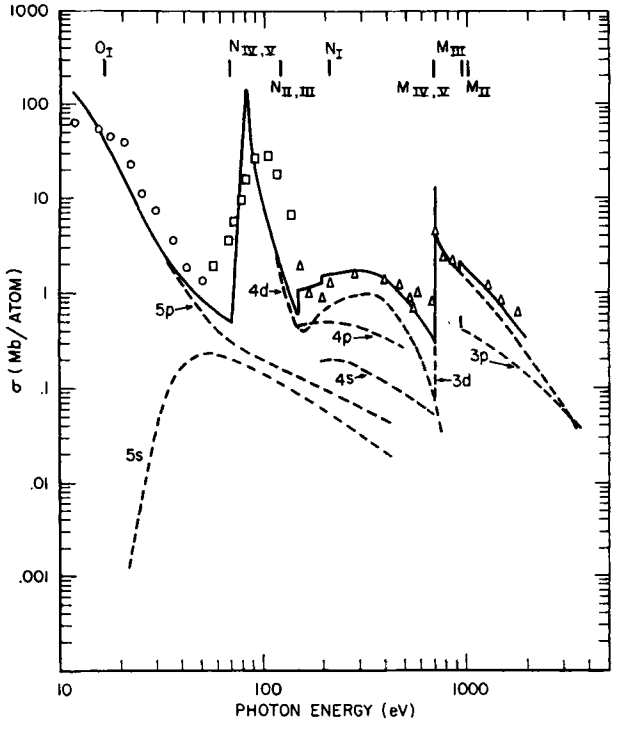

Fig. 1. Photoionization cross section of xenon. The total and subshell central field HS results[19] are shown in solid and dashed curves respectively, and the experimental results are shown as circles,[22] squares,[24] and triangles.[23]

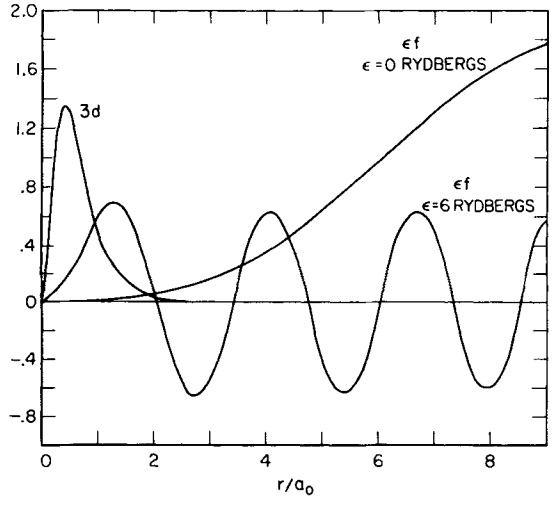

Fig. 2. The normalized 3d and εf HS central field wave functions for krypton.[19]

functions for the 3d → εf transition in krypton[19] are shown in Fig. 2 for two different continuum energies where the "penetration" of the continuum wave function with increasing energy is clearly seen.

Another feature shown in Fig. 1 is a minimum in a subshell cross section (and indeed in the total cross section) for the 4d subshell at $h\nu \approx 140$ eV. This minimum, known as a Cooper minimum,[25,26] is caused by the complicated overlap between discrete and continuum wave functions in the $l \rightarrow l + 1$ transitions of outer and near outer subshells whose wave functions are not nodeless, i.e., not 1s, 2p, 3d, or 4f. When the overlap is such that the positive contributions to the matrix element just cancel the negative contributions, a zero occurs in the $l \rightarrow l + 1$ dipole matrix element. In general it is not a zero minimum, even in the subshell cross section, because the degenerate $l \rightarrow l - 1$ transition matrix element does not vanish.

In any case, it is seen from Fig. 1 that the HS calculation does a reasonable job of reproducing both the delayed maxima and the Cooper minimum. In fact, it is quite good in the region between about 150 eV and 700 eV where the dominant contribution to the total cross section comes from the second maximum in the 4d cross section.

The discrepancies between theory and experiment near the thresholds are due to the fact that correlation is not included and that exchange is included only approximately via a central field. Before proceeding to a discussion of more exact treatments of photoionization, it is worthwhile to point out how the central field model applies to photoionization of ions.

For ions, there are only a very few photoionization measurements for singly charged ions[21] (Li^+, Na^+, and Ar^+) and none at all for multicharged ions. Despite this lack of experimental information, some general idea of the accuracy of central field calculation can be obtained by extrapolation from the neutrals. Looking at the Hamiltonian for an atom or ion with nuclear charge Z,

$$H = \sum_i \left(\frac{P_i^2}{2m} - \frac{Ze^2}{r_i}\right) + \sum_{i \neq j} \frac{e^2}{r_{ij}} \quad , \qquad (15)$$

we note that it is the last term, the interelectron repulsion, that is a non-central force so it is just this term that is being approximated in a central field model. Noting further that $1/r_i$ and $1/r_{ij}$ vary as Z, roughly speaking, then the central nuclear attraction goes as $\sim Z^2$ while the non-central term goes as $\sim Z$. Thus the ratio of the non-central to the central potential is $\sim 1/Z$ so that going along an isoelectronic sequence, i.e., increasing Z with a constant number of electrons, the non-central term becomes a smaller part of the total Hamiltonian. Since this is the very term being approximated, the approximation gets better for ions as opposed to atoms.[17] Thus we conclude that central field calculations will give about ±20% accuracy for atoms away from threshold features such as delayed maxima and Cooper minima; in the vicinity of the features the accuracy will be only a factor of two. For ions, the situation improves slowly as we go to higher and higher charge states for reasons described above as well as the fact that the various features move below threshold with increasing stage of ionization. A tabulation of total cross sections for all atoms and ions with $Z \leq 30$ predicted by the HS central field calculation has been published.[21]

IV. HARTREE-FOCK CALCULATIONS

The simplicity of wave functions consisting of single Slater determinants[28], i.e., antisymmetric products of one-electron functions, can be maintained while still treating exchange correctly. This is the Hartree-Fock (HF) method.[29] For calculations of discrete state wave functions, the method has been reviewed by Hartree[29,30] and Slater[28] among others. In addition, recent tabulations of extensive sets of HF discrete state wave functions have been reported.[31] Basically the method involves setting up a wave function ψ for the system in question, which is an antisymmetric product of one-electron functions, $r^{-1}P_{nl}(r)Y_l^m(\Theta,\Phi)$, or, more generally, a linear combination of such products so as to correctly resent the angular momentum couplings of many-electron system. The $P_{nl}(r)$ are treated as unknowns and the so-called energy functional

$\langle\Psi|H|\Psi\rangle$ is constructed; H is the exact nonrelativistic Hamiltonian. The variation principle is then applied to this functional subject to the constraints of the orthonormality of the one-electron functions. This results in a set of self-consistent coupled integro-differential equations for the $P_{nl}(r)$ which can then be solved, yielding the HF wave functions for the given state. Note that the HF wave function is the most accurate independent-particle wave possible since it is obtained via the variation principle.

Dealing with the final continuum state resulting from the photoionization process is more difficult since the HF problem is not defined for wave functions containing continuum orbitals. This is because the HF method solves for each orbital in the field generated by the charge distribution of the other orbitals. The charge distribution for a continuum orbital is not defined since continuum orbitals are non-normalizable. Thus, one proceeds as follows: first a HF calculation for the residual ion core minus photoelectron is performed. This can be done by ordinary discrete state HF procedures as described above, although some extra care must be taken when the photoelectron comes from an inner shell and the ion core is in an excited state well above the ionization threshold.[32] This done, the core orbitals are forzen and the above HF procedure can be carried out for the total ion core plus photoelectron final state with only the radial part of the continuum orbital, $P_{\varepsilon l}(r)$, unknown. This procedure yields a single integrodifferential equation for $P_{\varepsilon l}(r)$ which is known as the continuum HF equation. The details of this method for various cases are given elsewhere.[33-36]

As an example of the accuracy of the HF method, Fig. 3 shows the situation for the total cross section in xenon,[36] just as was shown in Fig. 1 for the central field calculation. Here we see that the agreement with experiment is considerably better than before, although there still are discrepencies in the regions close to the various thresholds, but not longer a factor of two but only as bad as 40-50%. Further the difference between "length" and "velocity" results really do give an indication of the accuracy of the calculated cross sections. Thus HF represents a considerable improvement over a central field calculation, showing the importance of the exchange interaction. The remaining discrepencies are due to the neglect of correlation, which must be included either explicitly or via multiconfiguration wave functions for quantitative accuracy near the outer shell thresholds where delayed maxima and Cooper minima are exhibited. Where these features are not manifested, as in the case of neon[36] shown in Fig. 4, we find excellent agreement with experiment as well as excellent agreement between "length" and "velocity".

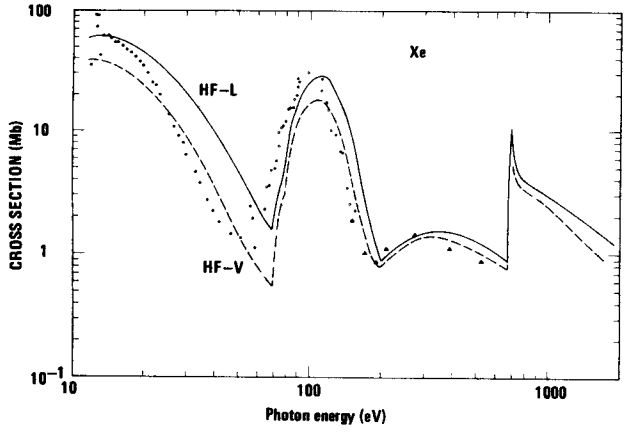

Fig. 3. Total photoionization cross section for Xe. The theoretical HF results in "length" and "velocity" approximations are shown[36] along with experimental results as in Fig. 1.

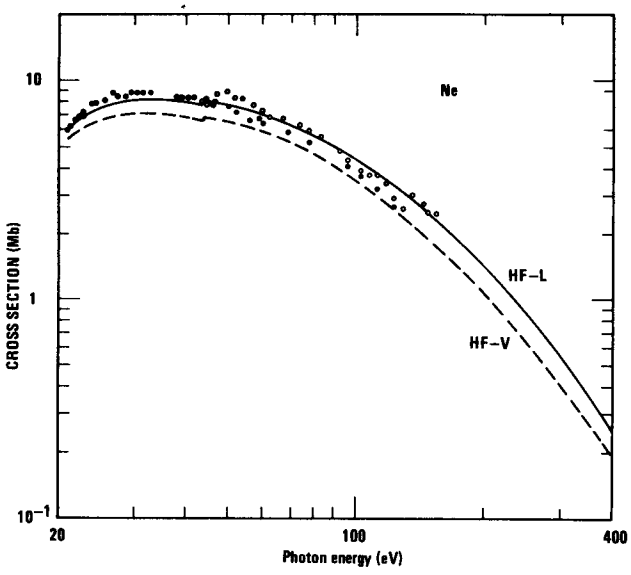

Fig. 4. Total photoionization cross section for Ne. The theoretical HF results in "length" and "velocity" approximations are shown[36] along with experimental results as in Fig. 1.

V. SOPHISTICATED CALCULATIONS

To go beyond the HF approximation, correlation must be included. The way this is generally done is by employing multiconfiguration wave functions for initial and final states of the system. There are a number of methodologies employed for these calculations which strive for quantitative accuracy, notably many-body-perturbation-theory (MBPT), the random phase approximation, (RPA), and R-matrix theory. MBPT is, as the name implies, a form of perturbation theory, developed some years ago.[37,38] It can in principle, be carried out to arbitrarily high order for as much accuracy as one might wish. It does however, have infinite sums as do all perturbation theories and so, in practice, approximations must be made, but it is still a very useful technique.[39,40] The RPA calculation is, in some ways, closely related to MBPT, although it can be derived in other ways also.[41,42] In essence RPA represents the sum to infinite order of certain classes of perturbation terms in MBPT, generally via the solution of coupled integro-differential equations.[43,44] Other classes of perturbation terms are omitted entirely, however. Thus, in a given situation, RPA may or may not be a useful technique, depending upon which perturbation terms are of importance. A further advantage of RPA is that the equality of "length" and "velocity" is preserved but, at present, its applicability is limited to closed shell systems.

The R-matrix method, as used,[45] is essentially a scheme in which the exact wave function is expanded in the large r region in a complete set (which is, of course, infinite) and truncated. Certain of the terms in the wave function, those referring to the continuum photoelectron, are left undetermined and they are obtained using a variational principle.[45,46] This might be considered multiconfiguration Hartree-Fock. In addition, in the inner region, the photoelectron is treated on the same footing as the bound electrons, and a different expansion is used. The inner and outer wave functions are joined at some intermediate value of r using the R-matrix.[45,47] The treatment of the wave function in the outer region is known as the close coupling approximation.[48] In this method the crucial point is which terms are to be included in the truncat-

ed summation.

As an example of the utility of these methods, the threshold region for the photoionization of argon is

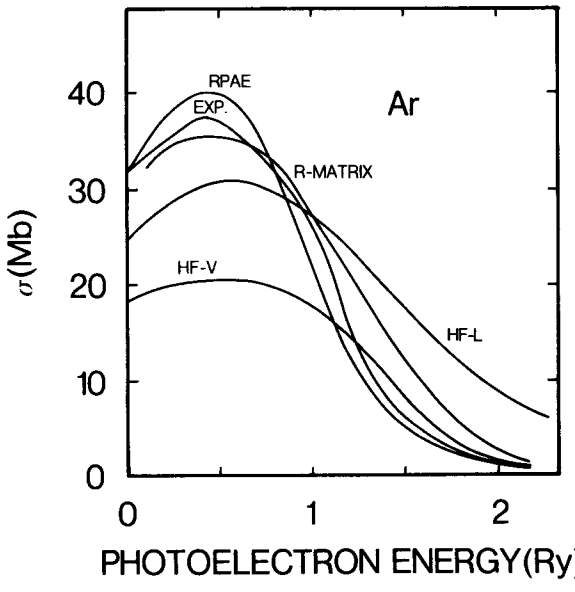

Fig. 5. Total photoionization cross section of argon. The theoretical RPA,[43] R-matrix,[45] and HF[36] results are shown along with the experimental[49,50] results.

ed summation.

As an example of the utility of these methods, the threshold region for the photoionization of argon is shown in Fig. 5 (note the linear scale) where it is seen that the HF results[36] are fair but both RPA[43] and R-matrix[48] give excellent agreement with experiment.[49,50]

In other instances, however, correlation can play a much larger role. This occurs particularly when the photoionization of a subshell with a small cross section is degenerate with one having a large cross section, i.e., when a given photon can ionize from both subshells, one with a much greater cross section. Such a case occurs for Ar 3s since it is so close to Ar 3p so that multiconfiguration effects are crucial. The situation is shown in Fig. 6 where is is seen that the

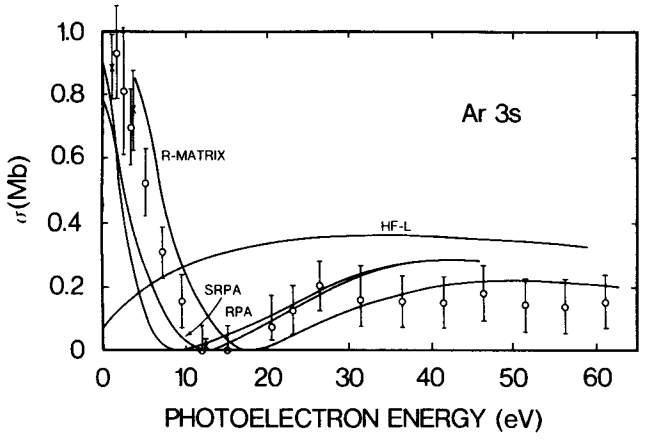

Fig. 6. Argon 3s subshell photoionization cross section. The theoretical RPA,[53] simplified SRPA,[54] R-matrix,[45] and HF[36] results are shown along with the experimental[51,52] results.

experimental cross section[51,52] has a Cooper minimum about 10 eV above threshold and these results are quite well represented by both R-matrix[48] and RPA[53,54] but not by the HF calculation[36] which shows no minimum. In a case like this, then, correlation must be included to get even qualitative agreement with experiment.

VI. APPLICATION TO SOLID PHOTOABSORPTION

Photoabsorption of core levels, i.e., inner shells in solids occurs on a distance scale small compared to atomic dimensions and, therefore, to first approximation, the solid state environment should not affect the photoionization very much. This idea has been scrutinized in considerable detail[55] and found to be generally true. As an example, consider the case of solid Au shown in Fig. 7. The atomic HS central field cross section[19,56] is compared with the measured results[57-59] in the solid. It is seen, from this comparison, that agreement is quantitatively excellent for $h\nu \geq 200$ eV and qualitatively quite good for 100 eV below that. This shows that simple atomic calculations can serve as useful first approximation to the photoionization of inner shells of solids. Since, however, the outer shell structure of an atom changes from its free state to the solid, thus changing the exchange and correlation interactions, the more sophisticated methods discussed above should not be applied unmodified to solids.

VII. ACKNOWLEDGEMENT

This work was supported by the U.S. Army Research Office.

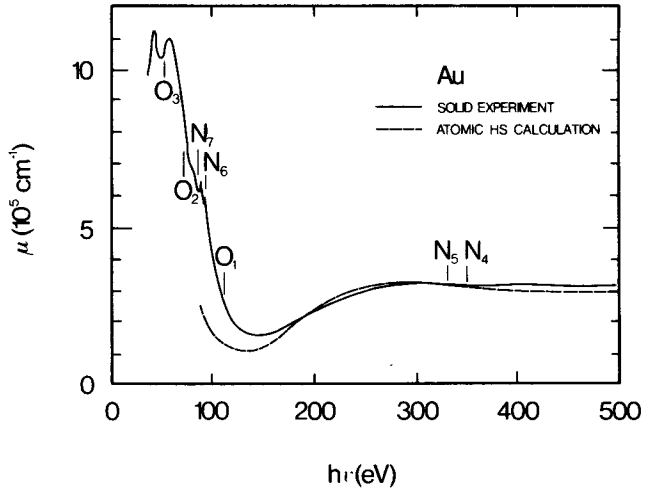

Fig. 7. Photoionization coefficient (proportional to the photoionization cross section) for gold. The dashed curve is the free atom HS central field result[19,56] and the solid curve is the experimental result[57-59] for solid gold.

REFERENCES

1. A. Einstein, Ann. Phys. (Leipzig) Ser. IV 17, 132 (1905).
2. H. A. Bethe in Handbuch der Physik, edited by H. Geiger and K. Scheel (Springer-Verlag, Berlin, 1933), Vol. 24/1, p. 482.
3. H. Hall, Rev. Mod. Phys. 8, 358 (1936).
4. S. T. Manson, Adv. Electronics Electron Phys. 41, 73 (1976).
5. S. T. Manson, Adv. Electronics Electron Phys. 44, 1 (1977).
6. S. T. Manson and D. Dill in Electron Spectroscopy, Theory, Techniques and Perspectives, edited by C. R. Brundle and A. D. Baker, (Academic Press, N.Y., 1978),

Vol. 2, p. 157.
7. A. F. Starace in Handbuch der Physik (in press).
8. J. A. R. Samson in Handbuch der Physik (in press).
9. D. R. Bates, Mon. Not. Roy. Astron. Soc. 106, 432 (1946).
10. H. A. Bethe and E. E. Salpeter, Quantum Mechanics of One and Two-Electron Atoms (Springer-Verlag, Berlin, 1957), pp. 247-323.
11. W. Heitler, Quantum Theory of Radiation (Oxford Univ. Press, London, 1954).
12. A. F. Starace, Phys. Rev. A 3, 1242 (1971).
13. A. F. Starace, Phys. Rev. A 8, 1141 (1973).
14. I. P. Grant, J. Phys. B 7, 1458 (1974).
15. I. P. Grant and A. F. Starace, J. Phys. B 8, 1999 (1975).
16. J. W. Cooper, Phys. Rev. 128, 681 (1962).
17. J. C. Slater, Phys. Rev. 81, 385 (1951).
18. F. Herman and S. Skillman, Atomic Structure Calculations (Prentice-Hall, Englewood Cliffs, N.J., 1963).
19. S. T. Manson and J. W. Cooper, Phys. Rev. 165, 126 (1968).
20. E. J. McGuire, Phys. Rev. 175, 20 (1968).
21. R. F. Reilman and S. T. Manson, Ap. J. Supp. 40, 815 (1979).
22. J. A. R. Samson, J. Opt. Soc. Am. 54, 842 (1964).
23. A. P. Lukirskii, I. A. Brytuv, and T. M. Zimkina, Opt. Specty. 17, 234 (1964).
24. D. L. Ederer, Phys. Rev. Lett. 13, 760 (1964).
25. U. Fano and J. W. Cooper, Rev. Mod. Phys. 40, 441 (1968).
26. J. W. Cooper, Phys. Rev. Lett. 13, 762 (1964).
27. A. Msezane, R. F. Reilman, S. T. Manson, J. R. Swanson, and L. Armstrong, Jr., Phys. Rev. A 15, 668 (1977).
28. J. C. Slater, Quantum Theory of Atomic Structure (McGraw-Hill, New York, 1960).
29. D. R. Hartree, The Calculation of Atomic Structures (Wiley, New York, 1957).
30. D. R. Hartree, Rep. Prog. Phys. 11, 113 (1946).
31. E. Clementi and C. Roetti, At. Data Nuc. Data Tables 14, 177 (1974).
32. P. S. Bagus, Phys. Rev. 139, A 619 (1965).
33. M. J. Seaton, Proc. Roy. Soc. Ser. A 208, 418 (1951).
34. A. Dalgarno, A. L. Stewart, and R. J. W. Henry, Planet. Space Sci. 12, 235 (1964).
35. M. Ya. Amusia, N. A. Cherepkov, L. V. Chernysheva, and S. I. Sheftel, Sov. Phys.-JETP 29, 1018 (1969).
36. D. J. Kennedy and S. T. Manson, Phys. Rev. A 5, 227 (1972).
37. J. Goldstone, Proc. Roy. Soc. Ser. A 239, 267 (1957).
38. K. A. Brueckner, The Many-Body Problem (Wiley, New York, 1959).
39. H. P. Kelly in Atomic Physics 2, edited by G. K. Woodgate and P.C.H. Sandars (Plenum, New York, 1971), p. 227.
40. H.P. Kelly in Atomic Inner Shell Processes edited by B. Crasemann (Academic, New York, 1975), Vol. I, p. 331.
41. G. Wendin in Photoionization and Other Probes of Many-Electron Interactions, edited by F. Wuilleumier (Plenum, New York, 1976), p. 61
42. T. N. Chang and U. Fano, Phys. Rev. A 13, 263 (1976).
43. M. Ya. Amusia, N. A. Cherepkov, and L. V. Chernysheva, Sov. Phys.-JETP 33, 90 (1971).
44. M. Ya. Amusia and N. A. Cherepkov, Case Studies in Atomic Physics 5, 47 (1976).
45. P. G. Burke and W. D. Robb, Adv. Atomic Molec. Phys. 11, 144 (1975).
46. W. Kohn, Phys. Rev. 74, 1963 (1948).
47. E. P. Wigner and L. Eisenbud, Phys. Rev. 72, 29 (1947).
48. P. G. Burke and K. T. Taylor, J. Phys. B 8, 2620 (1975).
49. J. A. R. Samson, Adv. Atomic Molec. Phys. 7. 179 (1966).
50. R. P. Madden, D. L. Ederer, and K. Codling, Phys. Rev. 177, 136 (1969).
51. J. A. R. Samson and J. L. Gardner, Phys. Rev. Lett. 33, 671 (1974).
52. R. G. Houlgate, J. B. West, K. Cooling, and G. V. Marr, J. Electron Spectrosc. 9, 205 (1976).
53. M. Ya. Amusia, N. A. Cherepkov, and L. V. Chernysheva, Phys. Lett. 40A, 15 (1972).
54. C. D. Lin, Phys. Rev. A 9, 171 (1974).
55. S.T. Manson, Topics in Applied Physics 26, 134 (1978).
56. F. Combet Farnoux and Y. Heno, Comptes Rend. 264B, 138 (1967).
57. P. Jaegle and G. Missoni, Comptes Rend. 262B, 71 (1966).
58. R. Haensel, C. Kunz, T. Sasaki, and B. Sonntag, Appl. Opt. 7, 301 (1968).
59. R. Haensel, K. Radler, B. Sonntag, and C. Kunz, Solid State Commun. 7, 1495 (1969).

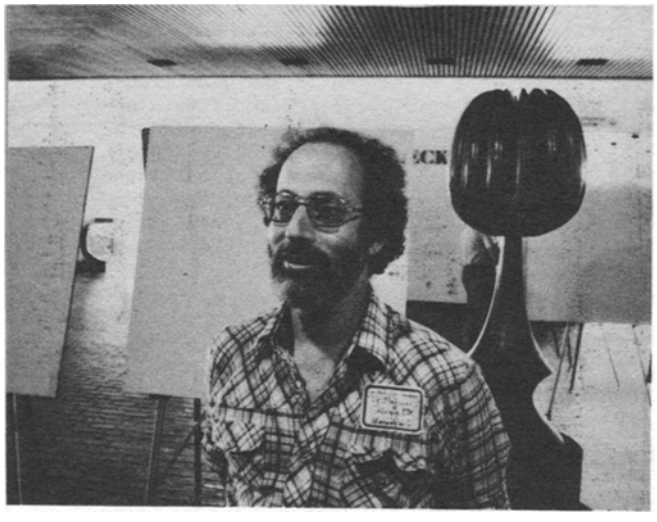

Dr. Steven Manson of Georgia State University, the conference's Theoretician in Residence, who coined the very valuable idea of theoretical "error bars".